

COMBINED EFFECTS OF NON-UNIFORM HEAT SOURCE/SINK AND RADIATION
ON HEAT TRANSFER OF A DUSTY FLUID OVER A STRETCHING SHEET

G. K. Ramesh & B. J. Gireesha^{1*}

*Department of Studies and Research in Mathematics, Kuvempu University,
Shankaraghatta-577 451, Shimoga, Karnataka, INDIA
E-mail: bjgireesu@rediffmail.com*

(Received on: 22-03-12; Accepted on: 09-04-12)

ABSTRACT

The present analysis consists of boundary layer flow and heat transfer of a dusty fluid over a stretching sheet in the presence of radiation and non uniform heat source/sink. Similarity transformation is used to simplify the governing equations. Here two different types of boundary heating are considered, namely PST and PHF. These equations are solved numerically by using Runge Kutta Fehlberg fourth-fifth order method (RKF45 Method). The effects of flow parameters like radiation, fluid particle interaction, non-uniform heat source/sink and Prandtl number on temperature distribution are studied. Comparison of the numerical results is made with previously published results under special cases, and the results are found to be in good agreement.

Key Words: *Boundary layer flow; dusty fluid; stretching sheet; radiation; non-uniform heat source; fluid-particle interaction parameter.*

AMS Subject Classification (2000): *76T15, 80A20;*

1. INTRODUCTION

Boundary-layer theory has been the working horse of modern fluid mechanics since its introduction to the engineering world which was given by Prandtl [19]. Over the past century, many engineering fluid mechanical problems have been solved using analytical and numerical methods. Specifically the flow of an incompressible boundary layer flow and heat transfer over a stretching sheet has important industrial applications, for example extrusion of plastic sheet, glass blowing, drawing plastic film, paper production, metal spinning and cooling of the metallic plate in a bath. Many authors investigated some mathematical results in the heat transfer problem. On this regard Sakiadis [17] has studied boundary layer problem generated by a continuous solid surface moving with a constant velocity. Crane [8] investigated the flow over a stretching sheet. Saffman [18] has discussed the stability of laminar flow of a dusty gas in which the dust particles are uniformly distributed.

Chakrabarti [10] analyzed the boundary layer in a dusty gas. N. Datta and S. K. Mishra [12] have investigated boundary layer flow of a dusty fluid over a semi-infinite flat plate. Further XIE Ming-liang, LIN Jianzhong and XING Fu-tang [15] have extended work of [12] and studied the hydrodynamic stability of a particle-laden flow in growing flat plate boundary layer. G. Palani and P. Ganesan [16] have studied heat transfer effects on dusty gas flow past a semi-infinite inclined plate. Agrawat [2] has studied dusty boundary layer flow and heat transfer, with the effect of pressure gradient. Chakrabarti and Gupta [9] have discussed the hydromagnetic flow and heat transfer over a stretching sheet.

Vajravelu and Nayfeh [21] analyzed the hydromagnetic flow of dusty fluid over a stretching sheet with the effect of suction and further the authors [22] gave a solution for flow and heat transfer in a second grade fluid over a stretching sheet. Tsai et.al [20] extended the work of Vajravelu and studied an unsteady flow over a stretching surface with non-uniform heat source. Abel et.al [3, 4] have studied the boundary layer flow and heat transfer in a viscoelastic fluid over a stretching sheet with prescribed surface temperature (PST case) and prescribed heat flux (PHF case). Further they studied radiation effect in a heat transfer analysis over a stretching sheet. Ishak et.al [14] have obtained the solution to unsteady laminar boundary layer over a continuously stretching permeable surface. Grubka and Bobba [13] have analyzed the stretching problem for a surface moving with a linear velocity and with variable surface temperature. Abdul Aziz [1] obtained the numerical solution for laminar thermal boundary over a flat plate with a convective surface boundary condition using the symbolic algebra software Maple and also found that similarity solution for the energy

***Corresponding author: B. J. Gireesha^{1*}, *E-mail: bjgireesu@rediffmail.com**

equation exists if the heat transfer coefficient h_f is proportional to $x^{-\frac{1}{2}}$, where x is the distance from the leading edge of the plate. This problem was then extended by Bataller [6, 5] to include the effect of radiation, and also to the Sakiadis flow. Bataller considered two sets of boundary conditions separately, for Blasius and Sakiadis flows. Chen [11] analyzed mixed convection of a power law fluid past a stretching surface in the presence of thermal radiation and magnetic field. Recently Gireesha et al. [7] obtained the numerical solution for boundary layer flow and heat transfer of dusty fluid over a stretching sheet with non-uniform heat source/sink.

Based on the above works, we intend to investigate the radiation effect on boundary layer flow and heat transfer of dust fluid over a stretching sheet taking into an account of non-uniform heat source/sink. Heat transfer analyses are examined for two types of boundary conditions, namely (i) wall is maintained with surface temperature and (ii) wall is maintained with heat flux. Numerical solutions for the flow and heat transfer are obtained using RKF45 method [1]. In the present paper we analyze the effect of radiation parameter, fluid-particle interaction parameter, Prandtl number, Eckert number and Non-uniform heat source/sink parameter.

2. FLOW ANALYSIS OF THE PROBLEM

Consider a steady two dimensional laminar boundary layer flow of a viscous dusty fluid over a stretching sheet. The sheet is coinciding with the plane $y = 0$, with the flow being confined to $y > 0$. Two equal and opposite forces are applied along the x -axis, so that the sheet is stretched, keeping the origin fixed. Both the fluid and the dust particle clouds are suppose to be static at the beginning. The dust particles are assumed to be spherical in shape and uniform in size.

The momentum equations of the two dimensional boundary layer flow in usual notation are [21]:

$$\frac{\partial u}{\partial x} + \frac{\partial v}{\partial y} = 0 \quad (2.1)$$

$$u \frac{\partial u}{\partial x} + v \frac{\partial v}{\partial y} = \nu \frac{\partial^2 u}{\partial y^2} + \frac{KN}{\rho} (u_p - u) \quad (2.2)$$

$$u_p \frac{\partial u_p}{\partial x} + v_p \frac{\partial u_p}{\partial y} = \frac{K}{m} (u - u_p) \quad (2.3)$$

$$u_p \frac{\partial v_p}{\partial x} + v_p \frac{\partial v_p}{\partial y} = \frac{k}{m} (v - v_p) \quad (2.4)$$

$$\frac{\partial}{\partial x} (\rho_p u_p) + \frac{\partial}{\partial y} (\rho_p v_p) = 0 \quad (2.5)$$

where (u, v) and (u_p, v_p) are the velocity components of the fluid and dust particle phases along x and y directions respectively. μ , ρ , ρ_p and N are the co-efficient of viscosity of the fluid, density of the fluid, density of the dust, number density of the particle phase, K is the stokes' resistance (drag co-efficient), m is the mass of the dust particle respectively. In deriving these equations, the drag force is considered for the iteration between the fluid and particle phases.

The boundary conditions for the flow problem is given by

$$\begin{aligned} u &= U_w(x), v = 0 \text{ at } y = 0, \\ u &\rightarrow 0, u_p \rightarrow 0, v_p \rightarrow v, \rho_p \rightarrow \omega\rho \text{ as } y \rightarrow \infty \end{aligned} \quad (2.6)$$

where $U_w(x) = cx$ is a stretching sheet velocity, $c > 0$ is stretching rate, ω is the density ratio. To convert the governing equations into a set of similarity equations, we introduce the following transformation as mentioned below,

$$\begin{aligned} u &= cx f'(\eta), v = -\sqrt{vc} f(\eta), \eta = \sqrt{\frac{c}{\nu}} y \\ u_p &= cx F(\eta), v_p = \sqrt{vc} G(\eta), \rho_r = H(\eta) \end{aligned} \quad (2.7)$$

which are identically satisfies (2.1), and substituting (2.7) into (2.2)-(2.5) we obtain the following non-linear ordinary differential equations.

$$f'''(\eta) + f(\eta)f''(\eta) - [f'(\eta)]^2 + l^*\beta H(\eta)[F(\eta) - f'(\eta)] = 0, \quad (2.8)$$

$$G(\eta)F'(\eta) + [F(\eta)]^2 + \beta[F(\eta) - f'(\eta)] = 0, \quad (2.9)$$

$$G(\eta)G'(\eta) + \beta[f(\eta) + G(\eta)] = 0, \quad (2.10)$$

$$H(\eta)F(\eta) + H(\eta)G'(\eta) + G(\eta)H'(\eta) = 0, \quad (2.11)$$

where a prime denotes differentiation with respect to η and $l^* = \frac{mN}{\rho}$, $\tau = m/k$ is the relaxation time of the particle phase, $\beta = \frac{1}{c\tau}$ is the fluid particle interaction parameter and $\rho_r = \frac{\rho_p}{\rho}$ is the relative density.

The boundary conditions defined as in (2.6) will become

$$\begin{aligned} f(\eta) = 0, f'(\eta) = 1 \text{ at } \eta = 0, \\ f'(\eta) = 0, F(\eta) = 0, G(\eta) = -f(\eta), H(\eta) = \omega \text{ as } \eta \rightarrow \infty. \end{aligned} \quad (2.12)$$

If $\beta = 0$ the analytical solution of (2.8) was given by Crane [8] as

$$f(\eta) = 1 - e^{-\eta} \quad (2.13)$$

obviously.

3. HEAT TRANSFER ANALYSIS

The governing dusty boundary layer heat transport equations in the presence of non-uniform heat source and radiation for two dimensional flow is [19],

$$u \frac{\partial T}{\partial x} + v \frac{\partial T}{\partial y} = \frac{k}{\rho c_p} \frac{\partial^2 T}{\partial y^2} + \frac{N}{\rho \tau_T} (T_p - T) + \frac{N}{\rho c_p \tau_v} (u_p - u)^2 + q''' - \frac{\partial q_r}{\partial y}, \quad (3.1)$$

$$u_p \frac{\partial T_p}{\partial x} + v_p \frac{\partial T_p}{\partial y} = -\frac{c_p}{c_m \tau_T} (T_p - T) \quad (3.2)$$

where T and T_p is the temperature of the fluid and temperature of the dust particle, c_p and c_m are the specific heat of fluid and dust particles, τ_T is the thermal equilibrium time and is time required by the dust cloud to adjust its temperature to the fluid, τ_v is the relaxation time of the of dust particle i.e., the time required by the a dust particle to adjust its velocity relative to the fluid, k is the thermal conductivity, q''' is the space and temperature dependent internal heat generation/absorption (non-uniform heat source/sink) which can be expressed as

$$q''' = \left(\frac{kU_w(x)}{xv} \right) [A^*(T_w - T_\infty)f'(\eta) + B^*(T - T_\infty)] \quad (3.3)$$

where A^* and B^* are the parameters of the space and temperature dependent internal heat generation/absorption. It is to be noted that A^* and B^* are positive to internal heat source and negative to internal heat sink, ν is the kinematic viscosity.

Using the Rosseland approximation for radiation [11], radiation heat flux is simplified as

$$q_r = -\frac{4\sigma^* \partial T^4}{3k^* \partial y} \quad (3.4)$$

where σ^* and k^* are the Stefan-Boltzman constant and the mean absorption co-efficient respectively. Assuming that the temperature differences within the flow such that the term T^4 may be expressed as a linear function of the temperature, we expand T^4 in a Taylor series about T_∞ and neglecting the higher order terms beyond the first degree in $(T - T_\infty)$ we get

$$T^4 \cong 4T_\infty^3 T - 3T_\infty^4 \quad (3.5)$$

Substituting (3.4) and (3.5) in (3.1) reduces to

$$\rho c_p \left(u \frac{\partial T}{\partial x} + v \frac{\partial T}{\partial y} \right) = \left(k + \frac{16\sigma^* T_\infty^3}{3k^*} \right) \frac{\partial^2 T}{\partial y^2} + \frac{Nc_p}{\tau_T} (T_p - T) + \frac{N}{\tau_v} (u_p - u)^2 + q''' \quad (3.6)$$

The solution of (3.6) and (3.2) depends on the nature of the prescribed boundary conditions. We employ two types of heating process as follows.

CASE-1: Prescribed Surface Temperature (PST-Case)

The prescribed surface temperature are defined in a quadratic function of x and is written as

$$T = T_w = T_\infty + A \left(\frac{x}{l}\right)^2 \text{ at } y = 0,$$

$$T \rightarrow T_\infty, T_p \rightarrow T_\infty \text{ as } y \rightarrow \infty. \quad (3.7)$$

where T_w and T_∞ denote the temperature at the wall and at large distance from the wall respectively. A is a positive constant, $l = \sqrt{\frac{\nu}{c}}$ is a characteristic length.

Defining the non-dimensional fluid phase temperature $\theta(\eta)$ and dust phase temperature $\theta_p(\eta)$ as

$$\theta(\eta) = \frac{T - T_\infty}{T_w - T_\infty}, \quad \theta_p(\eta) = \frac{T_p - T_\infty}{T_w - T_\infty}, \quad (3.8)$$

where $T - T_\infty = A \left(\frac{x}{l}\right)^2 \theta(\eta)$.

Using (3.7) and (3.8) into (3.2)-(3.6), we get

$$(1 + Nr)\theta''(\eta) + \text{Pr}[f(\eta)\theta'(\eta) - 2f'(\eta)\theta(\eta)] + \frac{NPr}{\rho c \tau_T} [\theta_p(\eta) - \theta(\eta)] + \frac{NPrEc}{\rho \tau_\nu} [F(\eta) - f'(\eta)]^2 + A^* f'(\eta) + B^* \theta(\eta) = 0, \quad (3.9)$$

$$2F(\eta)\theta_p(\eta) + G(\eta)\theta_p'(\eta) + \frac{c_p}{cc_m \tau_T} [\theta_p(\eta) - \theta(\eta)] = 0 \quad (3.10)$$

where $Pr = \frac{\mu c_p}{k}$ is the Prandtl number, $Ec = \frac{cl^2}{Ac_p}$ is the Eckert number, $Nr = \frac{16\sigma^* T_\infty^3}{3kk^*}$ is the Radiation parameter.

The boundary conditions for $\theta(\eta)$, $\theta_p(\eta)$ follows from (3.6) to (3.7) as

$$\theta(\eta) = 1 \text{ as } \eta = 0,$$

$$\theta(\eta) \rightarrow 0, \theta_p(\eta) \rightarrow 0 \text{ as } \eta \rightarrow \infty \quad (3.11)$$

CASE-2: Prescribed Heat Flux (PHF-Case)

In this case, the power law heat flux on the wall is considered in the form

$$-k \frac{\partial T}{\partial y} = q_w = D \left(\frac{x}{l}\right)^2 \text{ at } y = 0,$$

$$T \rightarrow T_\infty, T_p \rightarrow T_\infty \text{ as } y \rightarrow \infty \quad (3.12)$$

where D is the constant. On the other hand we define a non-dimensional fluid phase temperature $g(\eta)$ and dust phase temperature $g_p(\eta)$ as.

$$g(\eta) = \frac{T - T_\infty}{T_w - T_\infty}, \quad g_p(\eta) = \frac{T_p - T_\infty}{T_w - T_\infty} \quad (3.13)$$

where $T_w - T_\infty = \frac{D}{k} \left(\frac{x}{l}\right)^2 \sqrt{\frac{\nu}{c}}$.

Equations. (3.2)-(3.6) on using (3.12) and (3.13) can be transformed in terms of $g(\eta)$ and $g_p(\eta)$ as

$$(1 + Nr)g''(\eta) + \text{Pr}[f(\eta)g'(\eta) - 2f'(\eta)g(\eta)] + \frac{NPr}{\rho c \tau_T} [g_p(\eta) - g(\eta)] + \frac{NPrEc}{\rho \tau_\nu} [F(\eta) - f'(\eta)]^2 + A^* f'(\eta) + B^* g(\eta) = 0, \quad (3.14)$$

$$2F(\eta)g_p(\eta) + G(\eta)g_p'(\eta) + \frac{c_p}{cc_m \tau_T} [g_p(\eta) - g(\eta)] = 0 \quad (3.15)$$

where $Ec = \frac{kl^2c^2}{Dc_p\nu^2}$ is the Eckert number, and the boundary conditions becomes

$$g(\eta) = -1 \text{ as } \eta = 0,$$

$$g(\eta) \rightarrow 0, g_p(\eta) \rightarrow 0 \text{ as } \eta \rightarrow \infty \quad (3.16)$$

4. NUMERICAL SOLUTION

In the present work (2.8) to (2.11) are highly non-linear ordinary differential equations. To solve these equations we adopted symbolic algebra software Maple which was given by Aziz [1], and it is very efficient in using the well known Runge Kutta Fehlberg fourth-fifth order method (RKF45 Method) to obtain the numerical solutions of a boundary value problem. The system of boundary value problems of equations (2.8)-(2.12) and either (3.9)-(3.11) or (3.14)-(3.16) were solved by RKF45 method using the above mentioned software Maple. The RKF45 algorithm in Maple has been well tested for its accuracy and robustness.

5. RESULTS AND DISCUSSION

In the section we analyze boundary-layer flow and heat transfer of a dusty fluid over a stretching sheet in the presence of non-uniform source/sink, and the Rosseland approximation for the radiative heat flux is used. The temperature profile $\theta(\eta)$ and $\theta_p(\eta)$ in the PST case and $g(\eta)$ and $g_p(\eta)$ in the PHF case are depicted graphically in the presence of radiation and internal heat source/sink. A parameter of interest for the present study is the fluid particle interaction parameter β , Prandtl number Pr , Eckert number Ec , radiation Nr , space dependent heat source/sink A^* , temperature dependent heat source/sink B^* , Number density N .

In order to verify the accuracy of our present method, a comparison of wall temperature gradient $\theta'(0)$ with those reported by Abel and Mahesha [4] and Grubka and Bobba [13] for various values of Prandtl number. Either with the results of Vajravelu and Roper [22] and Tsai [20] for each value of B^* and Prandtl number. The result of this comparison is given in Table 1 and Table 2. The comparisons in all the above cases are found to be in excellent agreement. Sets of representative numerical results are illustrated graphically.

In Figure 1, is a graphical representation for the temperature distribution for PST and PHF case, for different values of β versus η . We infer from these figures that temperature of the fluid and dust phase decrease with increases in β respectively. Also it reveals that for the large values of β i.e., the relaxation time of the dust particle decreases then the velocities of both fluid and dust particle will be the same. We have used throughout our thermal analysis the values of $\tau_T = \tau_v = 0.5$ and $c_p = c_m = 0.2, \rho = 0.5, c = 1$.

Figure 2, illustrate variations of different values of Pr . By analyzing the graphs it reveals that the effect of increasing the Pr is to decreases the temperature distribution in the flow region in both PST and PHF cases, which implies that momentum boundary layer is thicker than the thermal boundary layer.

Figure 3, is plotted for the temperature distribution for PST and PHF case respectively, for different values of Ec . We observe that the effect of increasing values of Eckert number is to increase temperature of the fluid as well as temperature of dust phase. This is due to fact that the heat energy is stored in the considered liquid due to frictional heating.

Temperature profiles of the fluid and dust particle across the thermal boundary layer in the PST/PHF case are shown in Figure 4 for several values of A^* , it can be seen that the thermal boundary layer generates the energy, and this causes the temperature profiles increases with increases of $A^*(> 0)$ and decreases with increases of $A^*(< 0)$ Figure 5, depict the temperature profiles of the fluid and dust particle versus η for different values of B^* . The effect of B^* is similar to that given for A^* .

Figure 6, depict the temperature profiles for PST/PHF cases respectively. These figures shows the thermal radiation on temperature distributions in both cases, it observed that the increase in the thermal radiation parameter Nr produces a significant increases in the thickness of the thermal boundary layer fluid so the temperature distribution increases with increasing the value of Nr . Thus the radiation should be at its minimum in order to facilitate the cooling process.

Figure. 7 is plotted for the temperature profiles for different values of Number density of the dust particle N . It can be seen that the temperature profiles of fluid and dust particle decreases with increase of N . In all the figures, it is noticed that fluid phase temperature is higher than the dust phase temperature, which indicates that the fluid particle temperature is parallel to the dust particle temperature of both PST and PHF cases.

6. CONCLUSIONS

The present analysis includes the study of boundary layer flow and heat transfer of a dusty fluid over a stretching sheet in the presence of radiation and non uniform heat source/sink. Similarity transformations are used to transform the governing equations in to coupled nonlinear ordinary differential equations. Numerical solutions are obtained for the effect of thermal radiation and heat transfer of a dusty fluid over a stretching sheet in the presence of heat source or sink. The influence of several parameters like β , Pr , Ec , A^* , B^* and Nr on temperature profiles were examined. From our numerical results the following conclusions may be drawn

- Effect of thermal radiation parameter is to increase the temperature profile of both phases for both the cases of PST and PHF. Also the temperature increases in the presence of non-uniform heat source/sink.
- The rate of heat transfer $\theta'(0)$ is negative and $g(0)$ is positive.
- $\theta'(0)$ and $g(0)$ decreases with increasing the fluid-particle interaction parameter and Prandtl number.
- $\theta'(0)$ and $g(0)$ increases with increase in the radiation parameter, heat source or sink parameter and Eckert number.
- The effect of Prandtl number is to decrease the thermal boundary layer thickness.
- If $A^* \rightarrow 0, \beta \rightarrow 0, Nr \rightarrow 0$ and $N \rightarrow 0$ then our results coincides with the results of Vajravelu et.al., [21] and Tsai et.al., [20] when both Prandtl number and Heat source/sink varies.
- If $A^* \rightarrow 0, B^* \rightarrow 0, \beta \rightarrow 0, Nr \rightarrow 0$ and $N \rightarrow 0$ then our results with the results of Abel et.al., [4] and Grubka et.al., [13] only when Prandtl number varies.

REFERENCES

- [1] Abdul Aziz, A similarity solution for laminar thermal boundary layer over a flat plate with a convective surface boundary condition, *Com. Non. Sci Numer Simulat*, 14 (2009): 1064-1068.
- [2] V. M. Agranat, Effect of pressure gradient on friction and heat transfer in a dusty boundary layer, *Fluid Dynamics*, 23(5) (1988): 729-732.
- [3] M. S. Abel, P. G. Siddeshwar and Mahantesh M. Nandeppanavar, Heat transfer in a viscoelastic boundary layer flow over a stretching sheet with viscous dissipation and non-uniform heat source, *Int. J. of Heat and Mass Transfer*, 50 (2007): 960-966.
- [4] M. S. Abel and N. Mahesha, Heat transfer in MHD viscoelastic fluid flow over a stretching sheet with variable thermal conductivity, non-uniform heat source and radiation, *Applied Mathematical Modelling*, 32 (2008): 1965-1983.
- [5] R. C. Bataller, Radiation effects in the Blasius flow, *Appl. Math. Comput*, 198 (2008): 333-338.
- [6] R. C. Bataller, Radiation effects for the Blasius and Sakiadis flows with a convective surface boundary condition, *Appl. Math. Comput*, 206(2) (2008): 832-840.
- [7] B. J. Gireesha, G. K. Ramesh, M. Subhas Abel, C. S. Bagewadi, Boundary layer flow and Heat Transfer of a Dusty Fluid Flow over a Stretching Sheet with Non-uniform heat Source/Sink, *Int. J. of Multiphase Flow*, 37 (8)(2011): 977-982.
- [8] L. J. Crane, Flow past a stretching sheet, *Z. Angew. Math. Phys (ZAMP)*, 21 (1970): 645-647.
- [9] A. Chakrabarti and A. S. Gupta, Hydromagnetic flow and heat transfer over a stretching sheet, *Q. Appl. Math*, 37 (1979): 73-78.
- [10] K. M. Chakrabarti, Note on Boundary layer in a dusty gas, *AIAA Journal*, 12(8) (1974): 1136-1137.
- [11] C. H. Chen, MHD mixed convection of a power law fluid past a stretching surface in the presence of thermal radiation and internal heat generation/absorption, *Int. J. of Nonlinear Mechanics*, 44 (2008): 296-303.
- [12] N. Datta and S. K. Mishra, Boundary Layer Flow of a Dusty Fluid over a Semi-Infinite Flat Plate, *Acta Mechanica*, 42 (1982): 71-83.
- [13] L. J. Grubka and K. M. Bobba, Heat transfer characteristics of a continuous stretching surface with variable temperature, *J. Heat Transfer*, 107 (1985): 248-250.
- [14] A. Ishak, R. Nazar and I. Pop, Heat transfer over an unsteady stretching permeable surface with prescribed wall temperature, *Non-linear Analysis, Real World Applications*, 10 (2009): 2909-2913.
- [15] XIE Ming-liang, LIN Jian-zhong and XING Fu-tang, On the hydrodynamic stability of a particle-laden flow in growing flat plate boundary layer, *J. of Zhejiang University SCIENCE A*, 8(2) (2007) : 275-284.
- [16] G. Palani and P. Ganesan, Heat transfer effects on dusty gas flow past a semi-infinite inclined plate, *Forsch Ingenieurwes*, 71 (2007): 223-230.
- [17] B. C. Sakiadis, Boundary layer behaviour on continuous solid surface, *A.I.Ch.E.J*, 7 (1961): 26-28.
- [18] P. G. Saffman, On the stability of laminar flow of a dusty gas, *J. of Fluid Mechanics*, 13 (1962): 120-128.
- [19] H. Schlichting, Boundary layer theory, *McGraw-Hill*, (1968).
- [20] R. Tsai, K. H. Huang and J. S. Haung, Flow and heat transfer over an unsteady stretching surface with non-uniform heat source, *Int. Com. in Heat and Mass Transfer*, 35 (2008): 1340-1343.
- [21] K. Vajravelu and J. Nayfeh, Hydromagnetic flow of a dusty fluid over a stretching sheet, *Int. J. of Nonlinear Mechanics*, 27 (1992): 937-945.

- [22] K. Vajravelu and T. Roper, Flow and heat transfer in a second grade fluid over a stretching sheet, *Int. J. of Non-linear Mechanics*, 34(6) (1999) : 1031-1036.

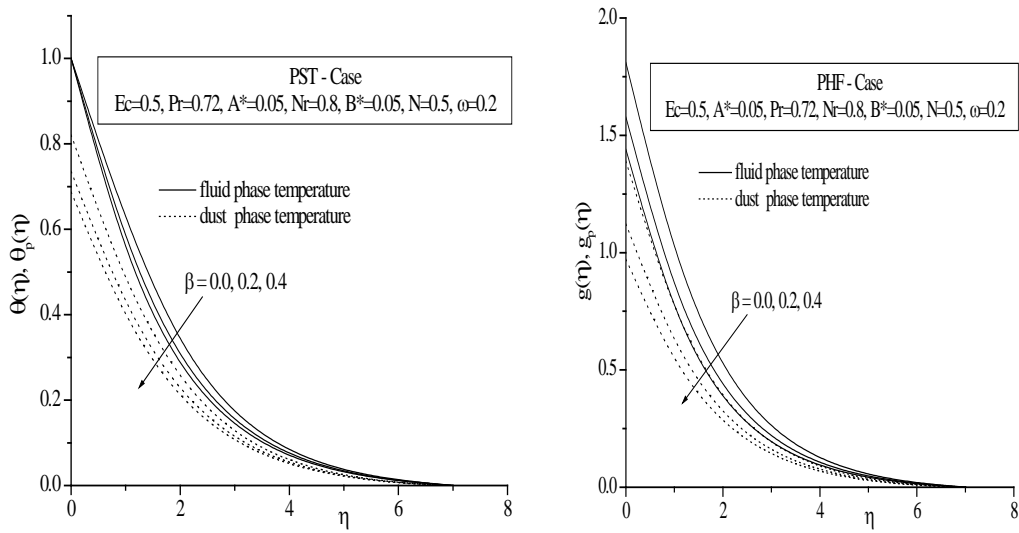


Figure-1: Effect of fluid-particle interaction parameter (β) on temperature distribution.

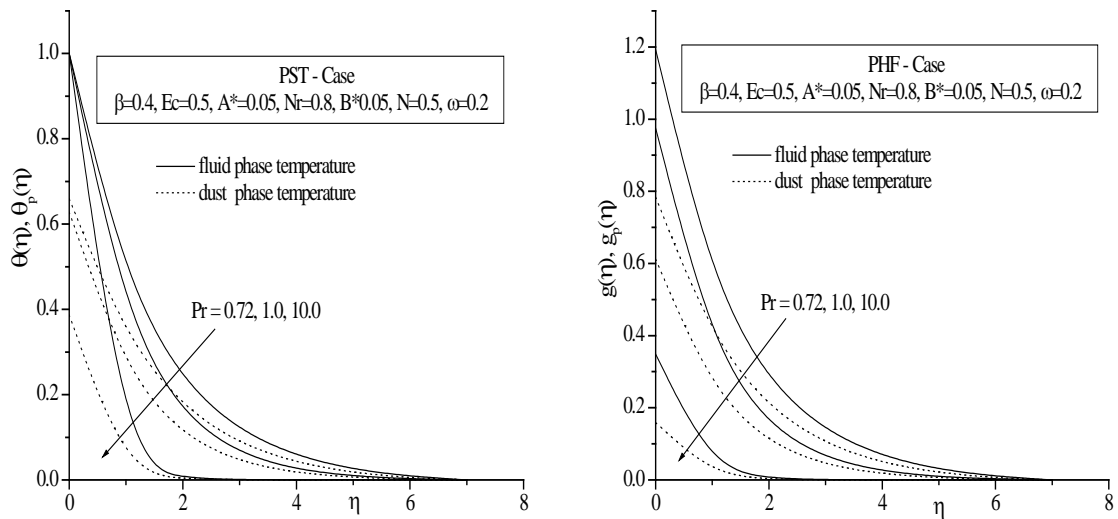


Figure-2: Effect of Prandtl number (Pr) on temperature distribution.

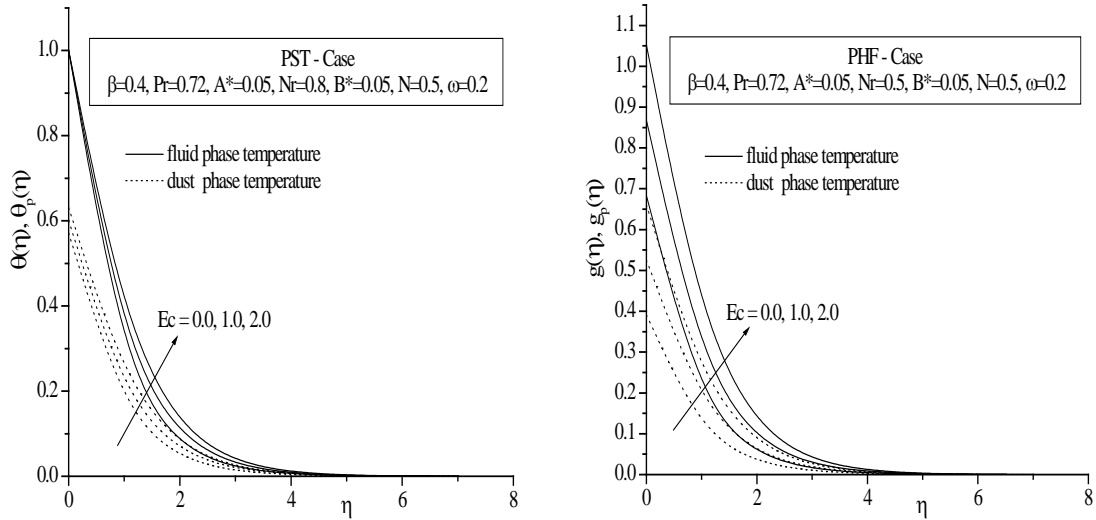


Figure-3: Effect of Eckert number (Ec) on temperature distribution.

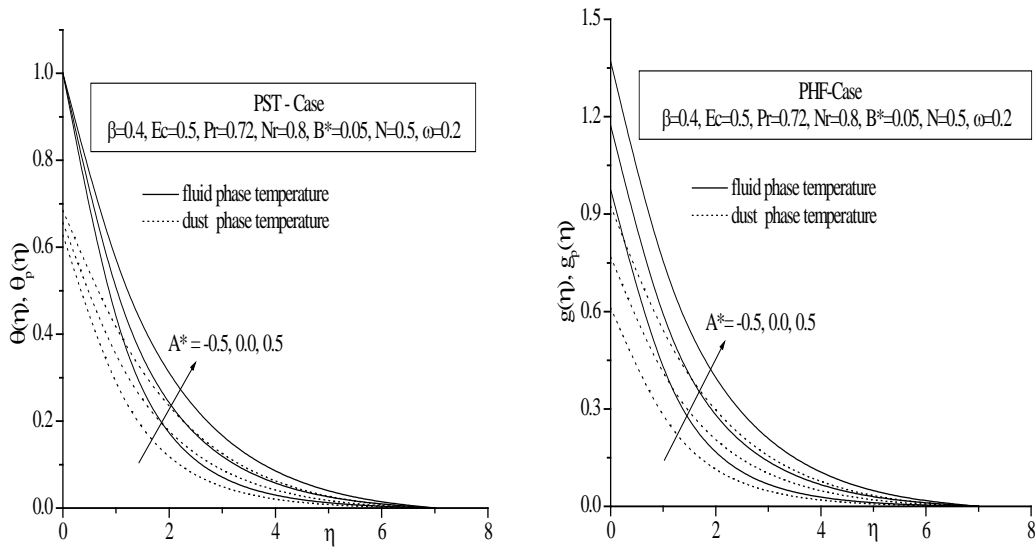


Figure-4: Effect of non-uniform heat source/sink (A^*) on temperature distribution.

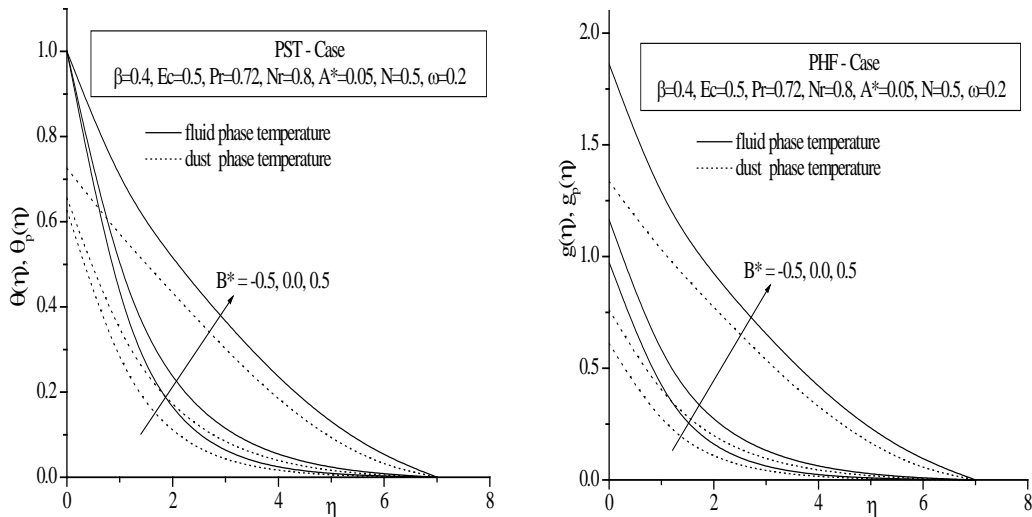


Figure-5: Effect of non-uniform heat source/sink (B^*) on temperature distribution.

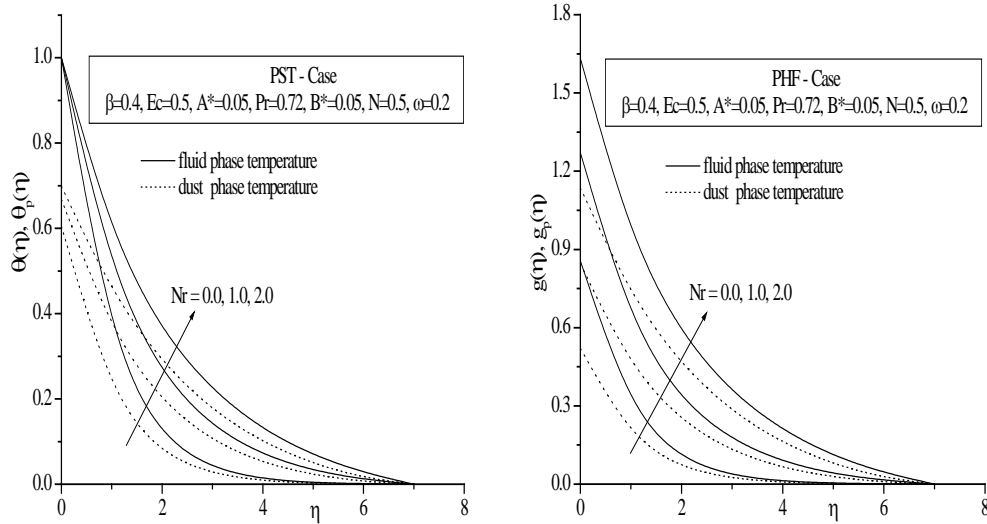


Figure-6: Effect of radiation parameter (Nr) on temperature distribution.

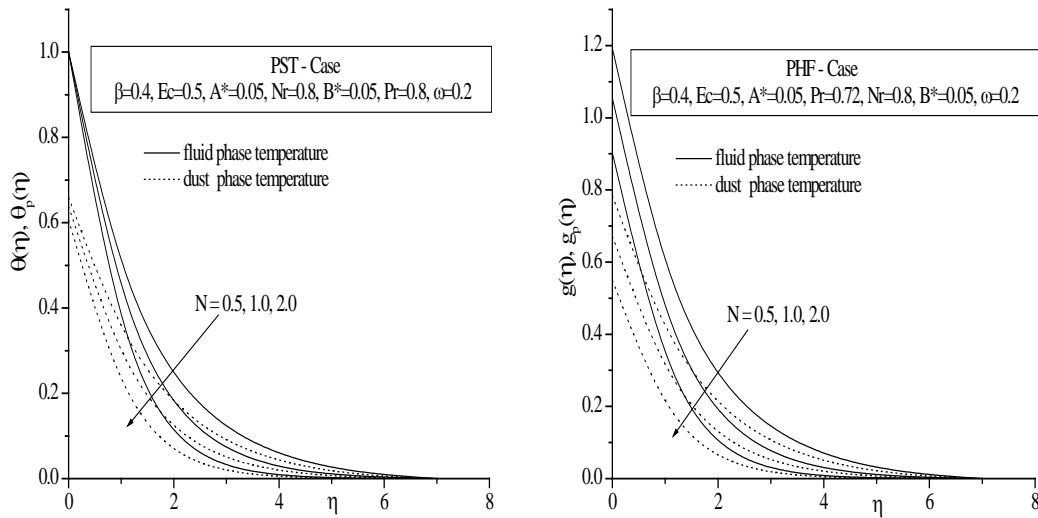


Figure-7: Effect of number density of the dust particle (N) on temperature distribution.

Table 1: Comparison results for the wall temperature gradient $-\theta'(0)$ in the case of $\beta = 0, A^* = 0, B^* = 0, Ec = 0, Nr = 0$ and $N = 0$.

Pr	Abel and Mahesha	Grubka and Bobba	Present Study
0.72	1.0885	1.0885	1.0889
1.0	1.3333	1.3333	1.3333
10.0	4.7969	4.7969	4.7969

Table 2: Comparison results for the wall temperature gradient $\theta'(0)$ in the case of $\beta = 0, A^* = 0, Ec = 0, Nr = 0$ and $N = 0$.

B^*	Pr	Vajravelu and Roper	Tsai et al.	Present Study
-2	2	-2.4860	-2.4859	-2.4859
-3	3	-3.0281	-3.0281	-3.0281
-4	4	-3.5851	-3.5851	-3.5851

Table 3: Wall temperature gradient $\theta'(0)$ and temperature function $g(0)$ for different values of the parameters $\beta, A^*, B^*, Ec, Pr, Nr = 0$ and N .

β	Ec	A^*	Pr	B^*	Nr	N	PST case $-\theta'(0)$	PHF case $g(0)$
0	2	0.05	0.72	0.05	3.0	0.5	0.205578	2.523035
0.2							0.312214	2.298003
0.4							0.376216	2.164802
0.4	0.0	0.05	0.72	0.05	3.0	0.5	0.526234	1.884670
	0.5						0.488730	1.954703
	2.0						0.376216	2.164802
0.4	2.0	-0.5	0.72	0.05	3.0	0.5	4.78432	1.973933
		0.0					0.385508	2.147451
		0.5					0.292584	2.320969
0.4	2.0	0.05	0.72	0.05	3.0	0.5	0.376216	2.164802
			1.0				0.463367	1.797290
			10.0				0.708026	1.271018
0.4	2.0	0.05	0.72	-0.5	3.0	0.5	0.539236	1.670068
				0.0			0.394228	2.096900
				0.5			0.142976	3.674200
0.4	2.0	0.05	0.72	0.05	1	0.5	0.561521	1.511346
					2		0.443269	1.857271
					3		0.376216	2.164802
0.4	2.0	0.05	0.72	0.05	3.0	0.5	0.376216	2.164802
					1		0.341371	2.023862
					2		0.273031	1.863659
